Journal of the Korean Physical Society, Vol. 73, No. 11, December 2018, pp. 1650∼1656

Dispersive Broadening of Two-photon Wave Packets Generated via Type-I and Type-II Spontaneous Parametric Down-conversion

Kang-Hee Hong, So-Young Baek,* Osung Kwon† and Yoon-Ho Kim‡
Department of Physics, Pohang University of Science and Technology (POSTECH), Pohang 37673, Korea

(Received 25 June 2018, in final form 13 July 2018)

Photons generated via spontaneous parametric down-conversion (SPDC) have broad spectrums and suffer from dispersive broadening of the temporal wave packets when they are transmitted through dispersive media. In this paper we theoretically and experimentally study the detailed amount of the temporal broadening of the two-photon wave packets generated via both type-I and type-II SPDC with β-BaB_2O_4 of various lengths, by transmitting them through optical fibers. We interpret the results with respect to the spectral properties of the two-photon wave packets. We believe that our results will contribute to implementing protocols involving long-range distributions of photon pairs.

PACS numbers: 42.65.Lm, 42.50.Dv, 41.20.Jb, 42.81.−i
Keywords: Parametric down-conversion, Dispersive broadening of two-photon wave packets, Second-order correlation function
DOI: 10.3938/jkps.73.1650

I. INTRODUCTION

The photon pair generated via spontaneous parametric down conversion (SPDC) has become a useful resource in quantum communication [1,2] and quantum computing [3]. The photon pair is used as a heralded single qubit source [4,5] or an entangled qubit source [6,7] in implementing various quantum information protocols. And many of these quantum information protocols require long range distribution of photons through optical fibers.

The photon pair generated via SPDC are spectrally correlated according to the phase matching condition of the process [8–10], and each photon usually has a broad spectrum even when they are generated by narrowband pumping. The broad spectrum of each photon causes the group velocity dispersion when it passes through dispersive media such as optical fibers.

Many studies have been done on the effect of dispersive broadening of the temporal wave packet of the photon pair generated via SPDC [11–14]. The temporal broadening of the two-photon wave packets also has been used in applications such as joint spectral intensity analysis of biphoton [15], and long-distance temporal quantum ghost imaging [16]. Research on the non-local manipulation or cancelation of the dispersion using non-local nature of the entangled photon pair generated via SPDC has been done as well [17–20].

In this paper we theoretically and experimentally investigate the detailed amount of the dispersive broadening effect on the photons generated via type-I and type-II SPDC process. We theoretically calculate the spectral properties of the photon pairs generated via type-I and type-II SPDC process with nonlinear media of different lengths. Additionally, we consider the effect of the spectral filtering on biphoton spectrum and simulate the spectral properties when each photon passes through the filters of different bandwidths. For the cases that the photon pairs pass through optical fibers of three different lengths, we simulate Glauber second order correlation functions [21]. We observe the dispersive broadening of the two-photon wave packets under aforementioned conditions experimentally by measuring relative coincidence counts as a function of time delay between the two photons, using a time correlated single photon counting (TCSPC) electronics. We reflect the transmission functions of the interference filters, the detection efficiency of the single-photon counters and the jitter time of the electronics to the Glauber second order correlation functions, and confirm that the experimental results agree well with the theoretical expectations.

II. EXPERIMENT

The scheme of the experiment to observe the dispersive broadening effect on photon pair generated via SPDC is

*Present address: Research Institute of Electrical Communication, Tohoku University, Sendai 980-8577, Japan
†Present address: National Security Research Institute, Daejeon 34044, Korea
‡E-mail: yoonho72@gmail.com

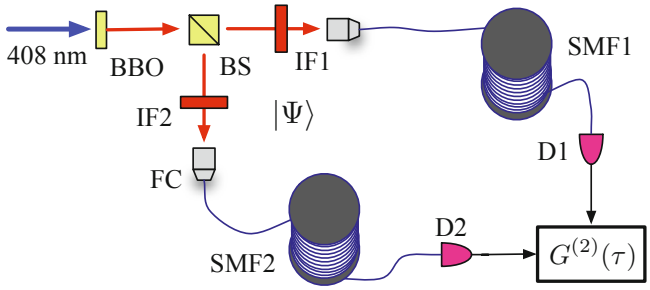

Fig. 1. (Color online) Schematic of the experiment. A type-I or type-II BBO crystal is pumped by a 408 nm diode laser. The signal-idler photon pair of the SPDC is split at the 50-50 beam splitter BS. IF1 and IF2 are spectral filters. The signal and the idler photons are entangled with the joint quantum state of $|\Psi\rangle$ and they are coupled into the single-mode optical fibers SMF1 and SMF2, respectively. The detection events at the detectors D1 at time t_1 and D2 at time t_2 are then analyzed to record the second order correlation function $G^{(2)}(t_1 - t_2) = G^{(2)}(\tau)$.

simple, see Fig. 1. The photon pair is generated via type-I or type-II SPDC process by pumping the crystals of which the optic axes are aligned so that the signal and idler photons propagate collinearly. The photons are split at the 50-50 beam splitter (BS) and are coupled into the single-mode optical fibers of identical lengths, SMF1 and SMF2, at each output of BS. Right before the fiber couplers we put the interference filters IF1 and IF2 to block the pump beam from coupling into the fibers. At the end of the fibers the photons are detected with the single photon counting modules D1 and D2. The temporal correlation of the two photons is measured from the number of coincidence events of the single photon detection of D1 at t_1 and of D2 at t_2. If the detectors and the other electronics are infinitely fast then the temporal correlation is measured to be proportional to the Glauber second order correlation function $G^{(2)}(t_1 - t_2) = G^{(2)}(\tau)$ [21].

Glauber second order correlation function is expressed as

$$G^{(2)}(t_1, t_2) = \left| \langle 0 | E_1^{(+)}(t_1) E_2^{(+)}(t_2) | \psi \rangle \right|^2, \quad (1)$$

where $|\psi\rangle$ is the state of the two-photon right after the BS and $E_1^{(+)}(t_1)$ and $E_2^{(+)}(t_2)$ are the positive frequency component of the quantized electric field operators at detector D1 and D2, which can be written as

$$E_1^{(+)}(t_1) = \int \mathrm{d}\omega f_1(\omega) \hat{a}_1(\omega) e^{i\frac{n(\omega)L_1}{c}\omega} e^{-i\omega t_1}, \quad (2)$$

and

$$E_2^{(+)}(t_2) = \int \mathrm{d}\omega f_2(\omega) \hat{a}_2(\omega) e^{i\frac{n(\omega)L_2}{c}\omega} e^{-i\omega t_2} \quad (3)$$

with the annihilation operators for each mode, $\hat{a}_1(\omega)$ and $\hat{a}_2(\omega)$, respectively. Here $f_1(\omega)$ and $f_2(\omega)$ represent the amplitude of the electric fields at D1 and D2, and $n(\omega)$ is the refractive index of the single-mode fiber. L_1 and L_2 are the lengths of the fibers and c is speed of light.

$f_1(\omega)$ and $f_2(\omega)$ are determined by the detection efficiency of the single photon counting modules and the transmission function of the filter in front of each detector. *i.e.*,

$$f_1(\omega) = S(\omega) F_1(\omega), \quad (4)$$

and

$$f_2(\omega) = S(\omega) F_2(\omega), \quad (5)$$

where $S(\omega)$ is the function describing the detection efficiency of the single-photon counting module [22] and $F_1(\omega)$ and $F_2(\omega)$ are the transmission functions of each filters in front of detector D1 and D2, respectively.

$n(\omega)$ is approximated up to frequency's first order expansion with respect to $\Omega_p/2$, the central frequency of the down-converted photons in degenerate case. *i.e.*,

$$n(\omega) \simeq n^{(0)} + n^{(1)} \times (\omega - \frac{\Omega_p}{2}). \quad (6)$$

In our case, the fused silica gives $n^{(0)} = n(\Omega_p/2) = 1.453$ and $n^{(1)} = \frac{\mathrm{d}n}{\mathrm{d}\omega}\big|_{\Omega_p/2} = 5.895 \times 10^{-18}$ for 408 nm pump beam.

1. Type-II SPDC process

The state of the photon pair generated via type-II SPDC process is described as follows [9,10],

$$|\psi(\omega_p)\rangle \sim \iint \mathrm{d}k_o \mathrm{d}k_e \int_0^L \mathrm{d}z \times e^{i\Delta z} \delta(\omega_o + \omega_e - \omega_p) \hat{a}^\dagger(\omega_e) \hat{a}^\dagger(\omega_o) |0\rangle, \quad (7)$$

where L is the length of the non-linear media. The subscript o and e refer to the signal and idler photons with horizontal and vertical polarizations, respectively, and the subscript p refers to the pump photon, of which the frequency ω_p originates from each mode of the multi-mode diode laser, centered at Ω_p. The phase mismatch between the pump, signal and idler photons is

$$\Delta = k_p - k_e - k_o. \quad (8)$$

By expanding the wave vectors in terms of frequencies, Eq. (8) can be written as the first order function of the frequencies as follows,

$$\Delta = -(\omega_p - \Omega_p) D_+ - \frac{1}{2}(\omega_o - \omega_e) D, \quad (9)$$

where the coefficients D_+ and D can be presented with the group velocities of the pump and the signal photons

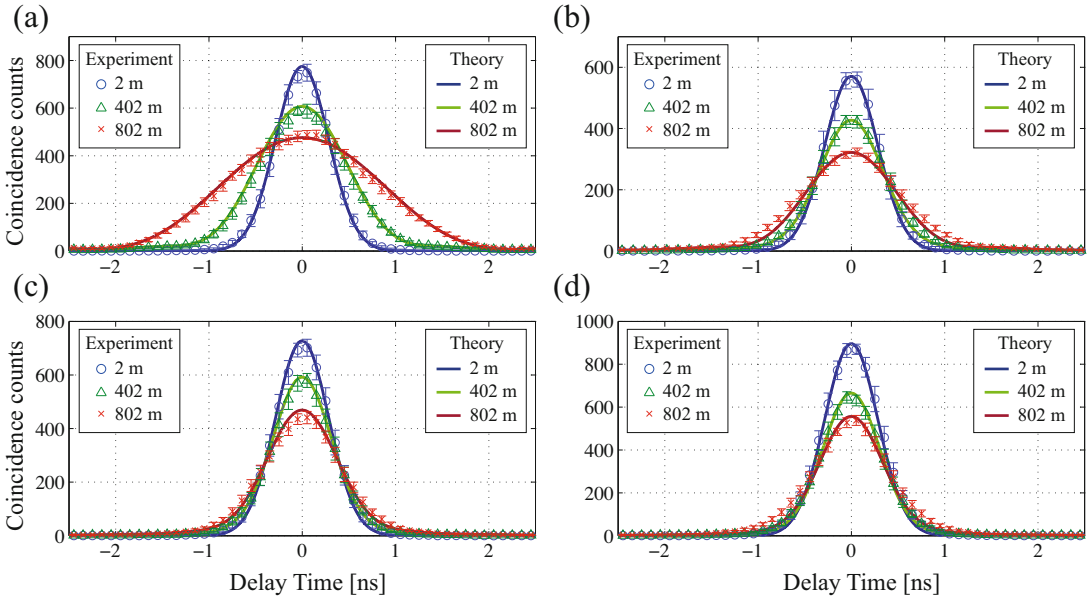

Fig. 2. (Color online) Experimental data (thin lines) and theoretical expectations (bold lines) for type-II SPDC with a (a) 1 mm BBO, (b) 2 mm BBO, (c) 3 mm BBO, and (d) 4 mm BBO. Both IF1 and IF2 have 80 nm FWHM bandwidth centered at 816 nm. The acquisition time for each of the data plot is (a) 100 s, 600 s, 2000 s, (b) 100 s, 250 s, 500 s, (c) 150 s, 450 s, 1000 s, and (d) 150 s, 300 s, 1000 s, respectively, for a 2 m, 402 m, 802 m long single-mode fiber spool in each path of the signal and the idler photons. The specific values of FWHM of the temporal wave packets in each plot under the effect of 2 m, 402 m, and 802 m of optical fibers are given as (a) 0.648 ns, 1.09 ns, and 1.85 ns, (b) 0.684 ns, 0.836 ns, and 1.20 ns, (c) 0.632 ns, 0.740 ns, and 0.936 ns, and (d) 0.696 ns, 0.728 ns, and 0.888 ns, respectively.

$u_o(\Omega)$ and of the idler photon $u_e(\Omega)$ at their central frequencies;

$$D_+ = \left[\frac{1}{u_o(\Omega_o)} + \frac{1}{u_e(\Omega_e)}\right] - \frac{1}{u_o(\Omega_p)}, \tag{10}$$

and

$$D = \frac{1}{u_o(\Omega_o)} - \frac{1}{u_e(\Omega_e)}. \tag{11}$$

The central frequencies of each down-converted photons Ω_o and Ω_e are equivalent to $\Omega_p/2$ for degenerate case.

$|\psi\rangle$ in Eq. (1) is the state after the BS, which is equivalent to the state that the BS's operation is applied to Eq. (7); *i.e.*,

$$\hat{a}(\omega) \to [\hat{a}_1(\omega) + \hat{a}_2(\omega)]/\sqrt{2}. \tag{12}$$

Finally, incoherent addition of the results of Eq. (1) for all ω_p weighting them according to the pump laser property gives us the temporal correlation of the photon pair generated via SPDC in which a non-linear media is pumped with a multi-mode diode laser [10]. Namely, the overall state can be described as follows,

$$\rho = \int \Phi(\omega_p) \mathrm{d}\omega_p |\psi(\omega_p)\rangle\langle\psi(\omega_p)| \tag{13}$$

where the spectral power density of the multi-mode diode laser is given as,

$$\Phi(\omega_p) \sim \sum_{n=-N}^{N} \exp\left[-\frac{(\omega_p - \Omega_p)^2}{2\sigma_p^2}\right] \delta(\omega_p - n\Delta\omega_p - \Omega_p), \tag{14}$$

with the bandwidth of the Gaussian profile σ_p and the mode spacing $\Delta\omega_p$.

We generate the photon pairs with various frequency correlations via SPDC with different lengths of nonlinear media, using type-II 1 mm, 2 mm, 3 mm and 4 mm β-BaB_2O_4 (BBO) crystals. We measure the temporal broadening of the photonic wave packets due to the dispersive media by observing the coincidence counts of detector D1 and D2 using two single-photon detectors and a time-correlated single-photon counting (TCSPC; PicoHarp 300, 4 ps resolution) device. The temporal broadening is measured for the dispersive media of different lengths by changing the lengths of SMF1 and SMF2 from 2 m to 402 m and to 802 m, adding one or two 400 m single-mode fiber spools to each path. We use the interference filters which have 80 nm full width half maximum (FWHM) of transmission spectral bandwidth centered at 816 nm for both IF1 and IF2. In our experiment we used 408 nm centered multi-mode diode laser with 0.3 nm spectral bandwidth and 0.03 nm mode spacing. We take the multi-mode effect into account in our theoretical simultations, which is found to be insignificant.

The results of the experiment are shown in Fig. 2, with the results from theoretical simulation. The small markers represent the experimental data, with error bars obtained by repeating the measurements 20 times. The thick solid lines are the results from theoretical simulations. Each plot in Figs. 2(a - d) shows the results of dispersive broadening of the photonic wave packets generated via using four different lengths of BBO crystals, 1 mm, 2 mm, 3 mm, and 4 mm, respectively.

Theoretically, a 2 m optical fiber is supposed to give almost no dispersive broadening effect on the photon pair. Indeed the ideal temporal FWHM of $G^{(2)}(t_1, t_2)$ with 2 m optical fibers derived from Eq. (1) and Eq. (7) is less than 4 ps, regardless of the length of the BBO crystal used here for the SPDC process. However, the blue data sets in Figs. 2(a - d) show temporal FWHM of 0.67 ns, on average. The reason that the temporal wave packets we get from the experiment have much broader width is the electronics timing jitter of the detectors. A realistic detector's response function is not a delta function, but a function with finite width. Therefore, the experimental result is not $G^{(2)}(t_1, t_2)$ but convolution of $G^{(2)}(t_1, t_2)$ and the detector's response function.

Although we do not know the detector's response function, we can deduce it from the experimental results using the fact that the convolution of a function with a delta function is the function itself. Because the FWHM of the ideal $G^{(2)}(t_1, t_2)$ is less than 4 ps for 2 m of optical fibers, and 4 ps is much narrower than the experimentally observed FWHM of 670 ps (the average of the blue data sets in Fig. 2), we approximate the ideal $G^{(2)}(t_1, t_2)$ as a delta function. Under this approximation, the experimental result, which is the convolution of the detector's response function and the delta function, is detector's response function itself. Based on this, we find the fitting function of each of the data set in Figs. 2(a - d) using 2 m of optical fibers and average the fitting parameters to get the detector's response function. The blue, green and red lines from theoretical simulations, are the results of convoluting the detector's response function and the ideal $G^{(2)}(t_1, t_2)$, each of which corresponds to the case of using 2m, 402 m and 802 m fibers, respectively.

Each plot in Fig. 2 shows that as the dispersive media gets longer the temporal wave packet gets broader. The specific values of FWHM of the experimental data sets in each plot of Fig. 2 under the effect of 2 m, 402 m, and 802 m optical fibers are given as (a) 0.648 ns, 1.09 ns, and 1.85 ns, (b) 0.684 ns, 0.836 ns, and 1.20 ns, (c) 0.632 ns, 0.740 ns, and 0.936 ns, and (d) 0.696 ns, 0.728 ns, and 0.888 ns, respectively. The plots show that the temporal waveform spreading of the photon pairs generated from the shorter crystals are the broader except for the cases using 2 m optical fibers, where the waveform spreadings entirely originate from electronics timing jitter of the detectors.

When long non-linear medium is used for SPDC process, the spectral property of the photon pair gets closer to the perfect phase matching condition; *i.e.* the spectrum of the two photon wave packet is concentrated in the state satisfying $\Delta = 0$ and $\omega_p = \omega_e + \omega_o$. This leads to the narrower spectral bandwidth of the down-converted photon pair. Figure 3 shows the normalized intensities of down-converted photon pairs from the perspective of the detectors, as a function of signal photon's wavelength. These normalized intensities is calculated based on Eq. (7), with Eq. (4) being also taken into account. The blue line in Fig. 3 represents the experimental condition of Figs. 2(a), green line (b), red line (c), and light blue (d), respectively. The FWHM of each intensity profile is given as 12.06 nm, 6.03 nm, 3.99 nm and 3.02 nm, respectively, showing the decrease in spectral bandwidth of the down-converted photon pair as the length of the non-linear medium increases. Since the filter with 80 nm FWHM centered at 816 nm works as a flat top filter in the range of the type-II SPDC spectrum, it is guaranteed that the IFs are not distorting the waveform of the type-II SPDC photon pair, while they keep the pump photon from entering into the single-photon detectors.

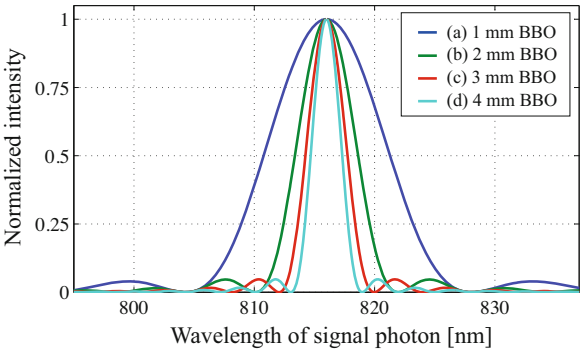

Fig. 3. (Color online) Theoretically derived normalized intensities of photon pairs generated via type-II SPDC under the experimental conditions. Each of the blue, green, red and light blue represent the normalized intensity of the photon pair generated from 1 mm, 2 mm, 3 mm, and 4 mm thick BBO crystals. The FWHM of each intensity profile is given as 12.06 nm, 6.03 nm, 3.99 nm and 3.02 nm, respectively.

2. Type-I SPDC process

The state of the photon pair generated via type-I SPDC process is described as follows [10],

$$|\psi(\omega_p)\rangle \sim \int \mathrm{d}k_s \mathrm{d}k_i \int_0^L \mathrm{d}z \times e^{i\Delta z}\delta(\omega_s + \omega_i - \omega_p)\hat{a}^\dagger(\omega_s)\hat{a}^\dagger(\omega_i)|0\rangle, \quad (15)$$

where L is the length of the non-linear medium. The subscript s and i refer to signal and idler photon, respectively. The phase mismatch between the pump, signal and idler photons generated via type-I SPDC process

is

$$\Delta = k_p - k_s - k_i. \tag{16}$$

Under the Taylor expansion of the wave vectors in terms of the frequencies, Eq. (16) can be written as the second order function of the frequencies as follows,

$$\Delta = (\omega_p - \Omega_p)D_p - \frac{1}{4}D''(\omega_s - \omega_i)^2, \tag{17}$$

where the coefficients D_p and D'' are given as

$$D_p = \left.\frac{\partial k_p}{\partial \omega}\right|_{\Omega_p} - \left.\frac{\partial k_s}{\partial \omega}\right|_{\frac{\Omega_p}{2}}, \tag{18}$$

and

$$D'' = \left.\frac{\partial^2 k_s}{\partial \omega^2}\right|_{\frac{\Omega_p}{2}}, \tag{19}$$

respectively.

After applying BS operation, Eq. (12), onto $|\psi(\omega_p)\rangle$ and substitute $|\psi\rangle$ in Eq. (1) with the result, we get the contribution of each pump mode of the multi-mode diode laser to $G^{(2)}(t_1, t_2)$. Incoherently adding the contributions for all ω_p weighting them according to Eq. (13) and Eq. (14) gives us the temporal correlation of the photon pair generated via SPDC using a multi-mode diode laser as a pump source [10].

The FWHM of the natural spectral bandwidth of the photon pair generated via type-I SPDC is much broader than that of the photon pair generated via type-II SPDC. Therefore, the IFs which are supposed to block the pump beam can distort the waveform of the photon pair generated via type-I SPDC because the spectrum of each photon is comparable to the IF's transmission spectrum. This means that due to the broad spectrum of the photon pairs, we can see the effect of IFs on dispersive broadening rather clearly. Here, we experimentally observe the dispersive broadening of the temporal wave packets of the photon pairs filtered with various IF configurations.

We generate the photon pairs using type-I BBO crystal of 3 mm length. We measure the temporal broadening of the photonic wave packets due to the dispersive media with three different IF configurations. Each IF configuration has transmission spectrum of the FWHM 80 nm both for IF1 and IF2; 80 nm for IF1 and 10 nm for IF2; 10 nm for both. The temporal broadening is measured for the dispersive media of different lengths by changing the lengths of SMF1 and SMF2 from 2 m to 402 m and to 802 m.

The results of the experiment are shown in Fig. 4, with the results from theoretical simulation. The plots in Figs. 4(a - c) show the results of dispersive broadening of the photonic wave packets generated via type-I SPDC with different IF configurations. Fig. 4(a) is when both IF1 and IF2 have 80 nm FWHM, (b) IF1 has 80 nm FWHM and IF2 10 nm FWHM, and (c) IF1 and IF2 both have 10 nm FWHM, respectively. The blue, green, and red colored data sets in each plot refer to the experimental situations with 2 m, 402 m, and 802 m fibers, respectively. In theoretical results represented by the solid lines in Fig. 4, we convolute the ideal $G^{(2)}(t_1, t_2)$ and the detector's response function that we found from approximation using the data in Fig. 2.

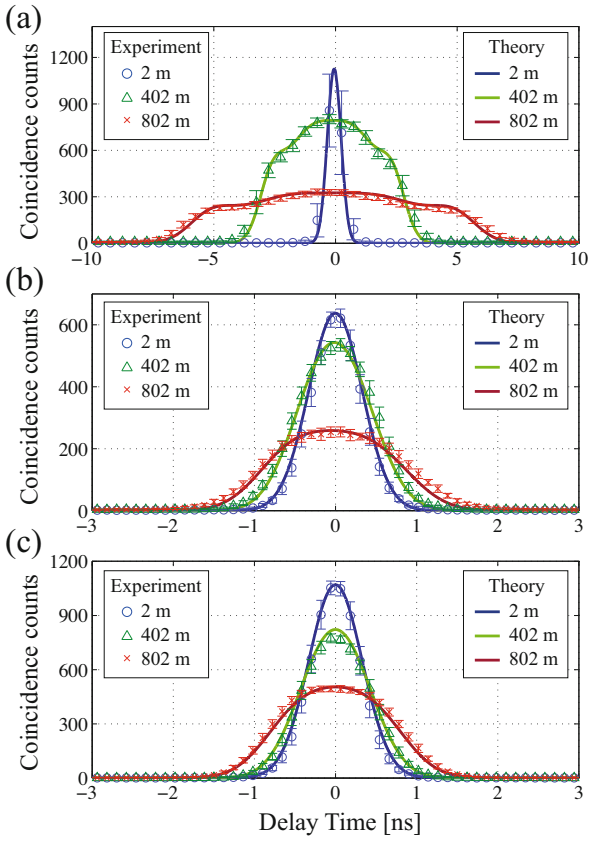

Fig. 4. (Color online) Experimental data (thin lines) and theoretical expectations (bold lines) with type-I SPDC for a 3 mm thick BBO. (a) IF1 and IF2 are 80 nm FWHM filters. (b) IF1 is 10 nm but IF2 80 nm FWHM. (c) Both IF1 and IF2 have 10 nm FWHM bandwidth. The acquisition time for each of the data plot is (a) 10 s, 100 s, 150 s, (b) 60 s, 120 s, 180 s, and (c) 100 s, 200 s, 1000 s, respectively, for a 2 m, 402 m, 802 m long single-mode fiber spool in each path of the signal and the idler photons. In this experiment, the natural bandwidth of type-I SPDC is roughly 80 nm. Note that spectrally filtering one of the photon pair is sufficient to reduce the spreading of the two-photon wave packet.The specific values of FWHM of the temporal wave packets in each plot under the effect of 2 m, 402 m, and 802 m of optical fibers are given as (a) 0.728 ns, 5.56 ns, and 11.4 ns, (b) 0.668 ns, 1.09 ns, and 1.99 ns, and (c) 0.692 ns, 1.01 ns, and 1.71 ns, respectively.

Each plot in Fig. 4 shows again that as the dispersive media gets longer the temporal wave packet gets broader. However, comparing the results using the photon pair generated via type-II SPDC the effect is magnified. The specific values of FWHM of the temporal wave packets

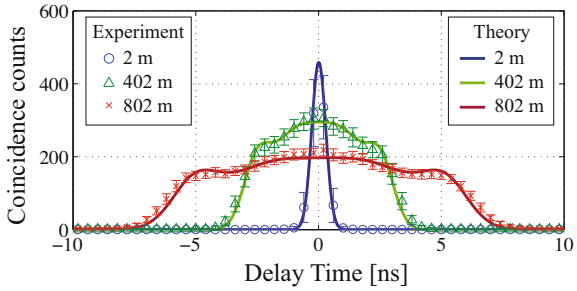

Fig. 5. (Color online) Experimental data (thin lines) and theoretical results (bold lines) for type-I SPDC with a 0.5 mm thick BBO. IF1 and IF2 are 80 nm FWHM filters. Since the filter bandwidth is much narrower than the natural bandwidth of SPDC, the biphoton wave packet dispersion is virtually identical to the 80 nm case shown in Fig. 4(a). The temporal spread of the wave packets are similar to that of the case in Fig. 4(a), where the specific values of FWHM of the temporal wave packets in each plot under the effect of 2 m, 402 m, and 802 m of optical fibers are given as 0.592 ns, 5.93 ns, and 11.7 ns, respectively.

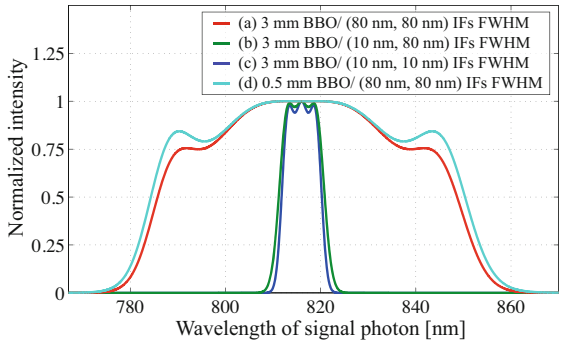

Fig. 6. (Color online) Theoretically derived normalized intensities of photon pairs generated via type-I SPDC under the experimental conditions. Red line represents the normalized intensity from the experimental condition corresponds to Figs. 4(a), green line (b), blue line (c), where all three are from 3 mm thick BBO crystal. Light blue line corresponds to that from 0.5 mm thick BBO (Fig. 5). The FWHM of each line is given as 9.70 nm, 11.04 nm, 72.37 nm, and 75.95 nm, respectively.

in each plot of Fig. 4 under the effect of 2 m, 402 m, and 802 m of optical fibers are given as (a) 0.728 ns, 5.56 ns, and 11.4 ns, (b) 0.668 ns, 1.09 ns, and 1.99 ns, and (c) 0.692 ns, 1.01 ns, and 1.71 ns, respectively. Comparison of Fig. 2(c) and Fig. 4(a), the results from which the photon pairs are generated using the same length of nonlinear medium and the same configuration of filters is used, shows that the spectrum of photon pair generated via type-I SPDC is much broader than that of via type-II.

Comparing Figs. 4(a) and (b), the spectral filtering on one photon dramatically reduces the dispersive broadening effect on the photonic wave packet. Meanwhile, comparing Figs. 4(b) and (c) shows the additional spectral filtering on the other photon does not change the spreading of the photonic wave packet very much. This is because of the spectral correlation of the down-converted photon pair, originated from the phase matching condition. Since we see the coincidence counts of the photon pair, spectrally filtering a frequency component ω_s on the signal photon automatically filters the idler photon's frequency component ω_i which has the correlation with ω_s. So the spectral filtering on only one side is sufficient to reduce the dispersive broadening effect of the photon pair generated via SPDC process [17].

The theoretically estimated value of the spectral bandwidth of the signal and idler photons generated from 3 mm thick BBO crystal from Eq. (15) is about 89 nm FWHM. This bandwidth is much broader than that of the 10 nm FWHM IFs. So for the cases that the IFs with 10 nm FWHM are used, we can guess that the results are reflecting the transmission function of the narrow filters clearly. However, since the spectral bandwidth is comparable to the transmission spectrum of the 80 nm FWHM IFs, it is possible that the resulting waveform can be distorted and not reflecting the filter's transmission function clearly. For next step, we generate the SPDC photon pair with broader frequency spectrum using 0.5 mm thick type-I BBO crystal, to see the effect of IFs with 80 nm FWHM on the dispersive broadening of photonic wave packets.

Figure 5 shows experimental and theoretical results of dispersive broadening of the two-photon wave packets generated via type-I SPDC using 0.5 mm thick BBO crystal, with 80 nm FWHM filters for both IF1 and IF2. The natural spectral bandwidth of the down-converted photon pair from 0.5 mm thick BBO is about 95 nm FWHM, which is broader than the transmission spectrum of the 80 nm IF. Therefore the two-photon waveform can be effectively considered as the same as the transmission function of the 80 nm filter. The specific values of FWHM of the temporal wave packets in each plot under the effect of 2 m, 402 m, and 802 m of optical fibers are given as 0.592 ns, 5.93 ns, and 11.7 ns, respectively, which are slightly broader than that of Fig. 4(a).

The results can be interpreted from the spectral property of the photon pair generated under each experimental conditions. Figure 6 shows the normalized intensities of photon pairs generated via type-I SPDC under each experimental conditions. The red, green and blue lines in Fig. 6 show the spectral properties of the photon pairs generated from 3 mm thick BBO crystal, where red is the result of filtering with IF1 = IF2 = 80 nm, green with IF1 = 10 nm and IF2 = 80 nm, blue with IF1 = IF2 = 10 nm. The red corresponds to Figs. 4(a), green (b), and blue (c), respectively. Here we can check from the green and the blue lines that filtering only one of the photons and both of the photons give almost similar waveforms. The FWHM of each bandwidth is given as 9.70 nm, 11.04 nm, 72.37 nm, respectively.

The light blue line in Fig. 6 shows the spectral properties of the photon pairs generated from 0.5 mm thick BBO crystal, filtered with IF1 = IF2 = 80 nm corresponding to the experimental situation in Fig. 5. Whereas the natural bandwidth of the photon pair generated from 3 mm thick BBO crystal is comparable to the filter's transmission function, that from 0.5 mm thick BBO crystal is broader. Therefore the light blue line in Fig. 6 shows the undistorted transmission function of the 80 nm filters. The FWHM of the bandwidth of (d) is given as 75.95 nm, which is slightly broader than that of (a) (red line).

III. CONCLUSIONS

We theoretically and experimentally investigated dispersive broadening of the wave packets of the photon pair generated via spontaneous parametric down-conversion (SPDC) process. We checked that the temporal spreading of the photonic wave packets transmitting through dispersive media is getting broader as the length of dispersive media getting longer. We generated photon pairs via type-II SPDC process using various lengths of nonlinear crystals, and observed the relation between the amount of dispersive broadening effect and the length of the non-linear crystal. We also generated photon pairs via type-I SPDC and observed the dispersive broadening effect when the photon pair undergoes spectral filtering by means of various configuration of interference filters.

We analyzed the results of dispersive broadening associated with the spectral properties of the SPDC photon pair. The temporal wave packet of the photon pair with the broader frequency spectrum spreads more after the photons transmitting through optical fibers. In addition we observed that due to the frequency correlation between the photon pair, the spectral filtering of only one of the photon pair sufficiently reduces the dispersive broadening effect.

We believe that our results can contribute to implementing various quantum informational protocols using photons generated via SPDC process, by providing a precise description on dispersive broadening effect which can be observed when long-range communication is involved.

ACKNOWLEDGMENTS

This work was supported in part by the National Research Foundation of Korea (Grant No. 2016R1 A2A1A05005202 and Grant No. 2016R1A4A1008978) and KIST ORP.

REFERENCES

[1] N. Gisin, G. Ribordy, W. Tittel and H. Zbinden, Rev. Mod. Phys. **74**, 145 (2002).
[2] C. H. Bennett *et al.*, Phys. Rev. Lett. **70**, 1895-1899 (1993).
[3] P. Kok *et al.*, Rev. Mod. Phys. **79**, 135 (2007).
[4] A. Soujaeff *et al.*, Opt. Express **15**, 726 (2007).
[5] P. C. Humphreys *et al.*, Phys. Rev. Lett. **111**, 150501 (2013).
[6] Y-H. Kim, S. P. Kulik and Y. Shih, Phys. Rev. Lett. **86**, 1370 (2001).
[7] M. Aspelmeyer *et al.*, Science **301**, 621 (2003).
[8] D. N. Klyshko, *Photons and Nonlinear Optics* (Gordon and Breach, New York, 1988).
[9] M. H. Rubin, D. N. Klyshko and Y.H. Shih, Phys. Rev. A **50**, 5122 (1994).
[10] O. Kwon, Y-S. Ra and Y-H. Kim, Opt. Express **17**, 13059 (2009).
[11] A. Valencia, M.V. Chekhova, A. Trifonov and Y. Shih, Phys. Rev. Lett. **88**, 183601 (2002).
[12] G. Brida, M.V. Chekhova, M. Genovese, M. Gramegna and L.A. Krivitsky, Phys. Rev. Lett. **96**, 143601 (2006).
[13] G. Brida, M. Genovese, L. A. Krivitsky and M.V. Chekhova, Phys. Rev. A **75**, 015801 (2007).
[14] A. Barak and M. Segev, Phys. Rev. A **86**, 043838 (2012).
[15] M. Avenhaus, A. Eckstein, P. J. Mosley and C. Silberhorn, Opt. Lett. **34**, 2873 (2009).
[16] S. Dong, W. Zhang, Y. Huang and J. Peng, Sci. Rep. **6**, 26022 (2016).
[17] S-Y. Baek, O. Kwon and Y-H. Kim, Phys. Rev. A **78**, 013816 (2008).
[18] S-Y. Baek, Y-W. Cho and Y-H. Kim, Opt. Express **17**, 19241 (2009).
[19] G. Brida *et al.*, Phys. Rev. Lett. **103**, 193602 (2009).
[20] V. T. Company, A. Valencia, M. Hendrych and J. P. Torres, Phys. Rev. A **83**, 023824 (2011).
[21] R. J. Glauber, Phys. Rev. **130**, 2529 (1963); **131**, 2766 (1963).
[22] http://www.excelitas.com/Pages/Product/Single-Photon-Counting-Modules-SPCM.aspx.